AIAA JOURNAL
Vol. 39, No. 12, December 2001

Blended AUSM+ Method for All Speeds and All Grid Aspect Ratios

Jan Vierendeels,* Bart Merci,† and Erik Dick‡
Ghent University, B-9000 Ghent, Belgium

An AUSM-based discretization method, using an explicit third-order discretization for the convective part and a line-implicit central discretization for the acoustic part and for the diffusive part, has been developed for incompressible and low-speed compressible Navier–Stokes equations. The lines are chosen in the direction of the gridpoints with shortest connection. The semi-implicit line method is used in multistage form because of the explicit third-order discretization of the convective part. Multigrid is used as acceleration technique. Because of the implicit treatment of the acoustic and the diffusive terms, the stiffness otherwise caused by high aspect ratio cells is removed. Low-Mach-number stiffness is treated by a preconditioning technique. To ensure physical correct behavior of the discretization for vanishing Mach number, extreme care has been taken. For vanishing Mach number, stabilization terms are added to the mass flux. Pressure and temperature stabilization terms are necessary. The coefficients of these terms are chosen so that correct scaling with Mach number is obtained. A blend of the low-speed algorithm with the original AUSM algorithm developed for high-speed applications has been constructed so that the resulting algorithm can be used at all speeds.

Introduction

PRECONDITIONING of the incompressible[1,2] and compressible Navier–Stokes equations for low-Mach-number flows[1–4] is frequently used to accelerate convergence. However, this technique does not always provide good results on high-aspect-ratio grids because of the stiffness introduced by the numerically anisotropic behavior of the diffusive and acoustic terms.

In our work, the stiffness due to the grid aspect ratio is removed by the use of a line method. The low-Mach-number stiffness is avoided by an appropriate discretization and a local preconditioning technique. Multigrid is used as convergence accelerator. The discretization is based on AUSM as developed by Liou and Steffen[5] and further extended to low-Mach-number applications by Edwards and Liou.[6] The preconditioning technique of Weiss and Smith[1] is employed.

The purpose of the work is to construct a scheme that reaches high quality and high efficiency independent of Mach number and grid aspect ratio. The focus of the present work is to demonstrate that an algorithm developed for incompressible and low-speed compressible flows can be combined with an algorithm developed for high-speed compressible flows. Results for a range of Mach numbers and for varying grid aspect ratios are given, demonstrating insensitivity of the computational efficiency to these parameters.

Incompressible Flow

Governing Equations

The two-dimensional steady Navier–Stokes equations in conservative form for an incompressible fluid are

$$\frac{\partial F_c}{\partial x}+\frac{\partial F_a}{\partial x}+\frac{\partial G_c}{\partial y}+\frac{\partial G_a}{\partial y}=\frac{\partial F_v}{\partial x}+\frac{\partial G_v}{\partial y}$$

where F_c and G_c are the convective fluxes, F_a and G_a are the acoustic fluxes, and F_v and G_v are the viscous fluxes:

$$F_c=\begin{bmatrix}0\\ u^2\\ uv\end{bmatrix},\qquad F_a=\begin{bmatrix}u\\ p'\\ 0\end{bmatrix},\qquad F_v=\begin{bmatrix}0\\ \nu\dfrac{\partial u}{\partial x}\\ \nu\dfrac{\partial v}{\partial x}\end{bmatrix}$$

$$G_c=\begin{bmatrix}0\\ uv\\ v^2\end{bmatrix},\qquad G_a=\begin{bmatrix}v\\ 0\\ p'\end{bmatrix},\qquad G_v=\begin{bmatrix}0\\ \nu\dfrac{\partial u}{\partial y}\\ \nu\dfrac{\partial v}{\partial y}\end{bmatrix}$$

where u and v are the Cartesian components of velocity, p' is the kinematic pressure ($p'=p/\rho$), p is the pressure, ρ is the density, and ν is the kinematic viscosity.

Discretization

We consider an orthogonal grid. The convective part of the equations is discretized with the third-order Van Leer-κ method.[7] The acoustic and viscous parts are discretized centrally. Because of the central discretization of the acoustic part, pressure stabilization is necessary.

The artificial dissipation term for the pressure, added to the viscous terms, is given by

$$F_{d_{i+\frac{1}{2}}}=\delta\frac{p'_{i+1}-p'_i}{\beta_x}\begin{bmatrix}1\\ u_{i+\frac{1}{2}}\\ v_{i+\frac{1}{2}}\end{bmatrix}$$

$$G_{d_{j+\frac{1}{2}}}=\delta\frac{p'_{j+1}-p'_j}{\beta_y}\begin{bmatrix}1\\ u_{j+\frac{1}{2}}\\ v_{j+\frac{1}{2}}\end{bmatrix}$$

where β_x and β_y have the dimension of velocity. We have taken

$$\beta_x=w_r+2\nu/\Delta x,\qquad \beta_y=w_r+2\nu/\Delta y \tag{1}$$

where w_r is a local or a global velocity and $\delta=\frac{1}{2}$. Full details on the discretization are given in Ref. 8.

Presented as Paper 2000-2255 at Fluids 2000, Denver, CO, 13–22 June 2000; received 14 July 2000; revision received 22 May 2001; accepted for publication 4 July 2001.

*Senior Researcher, Department of Flow, Heat and Combustion Mechanics, Sint-Pietersnieuwstraat 41. Member AIAA.

†Postdoctoral Fellow of the Fund for Scientific Research–Flanders (Belgium) (F. W. O.–Vlaanderen), Department of Flow, Heat and Combustion Mechanics, Sint-Pietersnieuwstraat 41. Member AIAA.

‡Professor, Department of Flow, Heat and Combustion Mechanics, Sint-Pietersnieuwstraat 41. Senior Member AIAA.

Time-Marching Method

Applying the pseudocompressibility method to the Navier–Stokes equations gives

$$\Gamma\frac{\partial \boldsymbol{Q}}{\partial \tau}+\frac{\partial F_c}{\partial x}+\frac{\partial F_a}{\partial x}+\frac{\partial G_c}{\partial y}+\frac{\partial G_a}{\partial y}=\text{right-hand side}$$

where $\boldsymbol{Q}$ is the vector of variables $[p', u, v]^T$. The preconditioning matrix Γ is given by

$$\Gamma=\begin{bmatrix}1/\beta^2 & 0 & 0\\ 0 & 1 & 0\\ 0 & 0 & 1\end{bmatrix} \tag{2}$$

where β has the dimension of velocity. The eigenvalues of the inviscid part of the preconditioned system are given by

$$\lambda\left[\Gamma^{-1}\frac{\partial(n_xF+n_yG)}{\partial \boldsymbol{Q}}\right]=w, w+c, w-c \tag{3}$$

where $w=n_xu+n_yv$, $c=\sqrt{(w^2+\beta^2)}$, and n_x and n_y are an arbitrary direction with $n_x^2+n_y^2=1$. If β is of the same order of magnitude as the convective speed, all eigenvalues are properly scaled at least in one direction.

This artificial-compressibility method is used as smoother for the multigrid. The artificial-compressibility method belongs to the family of local preconditioning techniques. Local preconditioning is known to work well on isotropic grids,[3] but not always on nonisotropic grids, with high aspect ratios. A semi-implicit discretization is needed to have a robust method suitable for high-aspect-ratio meshes.[8]

Stepping in Pseudotime

A multistage stepping is used with four stages:

$$\boldsymbol{Q}_0=\boldsymbol{Q}^n,\qquad \boldsymbol{Q}_1=\boldsymbol{Q}_0+\alpha_1\,\text{CFL}\,\Delta\boldsymbol{Q}_0$$
$$\boldsymbol{Q}_2=\boldsymbol{Q}_0+\alpha_2\,\text{CFL}\,\Delta\boldsymbol{Q}_1,\qquad \boldsymbol{Q}_3=\boldsymbol{Q}_0+\alpha_3\,\text{CFL}\,\Delta\boldsymbol{Q}_2$$
$$\boldsymbol{Q}_4=\boldsymbol{Q}_0+\alpha_4\,\text{CFL}\,\Delta\boldsymbol{Q}_3,\qquad \boldsymbol{Q}^{n+1}=\boldsymbol{Q}_4 \tag{4}$$

with $\{\alpha_1,\alpha_2,\alpha_3,\alpha_4\}$ equal to $\{\frac{1}{4},\frac{1}{3},\frac{1}{2},1\}$ and the Courant–Friedrichs–Lewy (CFL) number equal to 1.8. We denote this CFL number as the global CFL number of the method. The $\Delta\boldsymbol{Q}$ of each stage is computed with the semi-implicit line method, shown in Eq. (8).

The multistage semi-implicit method is accelerated with the multigrid technique. A full approximation scheme is used in a W cycle with four or five levels of grids. The computation is started on the finest grid to show the full performance of the multigrid method. For the restriction operator, full weighting is used. The prolongation is done with bilinear interpolation. Two pre- and postrelaxations are done. The use of five levels of grids results in a cost of 32.375 work units for each multigrid cycle, when one work unit consists of a residual evaluation and an update, or a residual evaluation together with a restriction and a prolongation.

Determination of the Pseudotime Step

Consider a uniform Cartesian mesh with constant Δx and Δy. The time step $\Delta\tau$ on this mesh is computed as

$$\Delta\tau=1/[(|u|+c_x)/\Delta x+(|v|+c_y)/\Delta y] \tag{5}$$

with

$$c_x=\sqrt{(u^2+\beta^2)},\qquad c_y=\sqrt{(v^2+\beta^2)} \tag{6}$$

Assume that the flow is inviscid and aligned to the x direction, that is, $v=0$. If β is chosen in the order of u, then all three eigenvalues (3) have the same order of magnitude in the x direction and all waves are convected into this direction with comparable speed. The ideal situation is reached for a CFL number in the order of unity.

If the allowable CFL number becomes smaller, the convergence breaks down. This happens for large grid aspect ratios. We define the grid aspect ratio g_{ar} for the Cartesian grid as

$$g_{\text{ar}}=\Delta x/\Delta y$$

If g_{ar} is very large, then the allowable time step $\Delta\tau$ is equal to $\Delta y/c_y$, and the maximum allowable CFL number in the x direction is

$$\text{CFL}_x=\frac{(|u|+c_x)\Delta\tau}{\Delta x}=\frac{|u|+c_x}{c_y}\frac{1}{g_{\text{ar}}}\approx\frac{1}{g_{\text{ar}}}$$

If the acoustic fluxes in the y direction are discretized implicitly, the system stays stable if the time step definition is changed into

$$\Delta\tau=1/[(|u|+c_x)/\Delta x+\omega_1|v|/\Delta y] \tag{7}$$

where ω_1 is a scaling factor[8] set equal to 2. This corresponds with $c_y=|v|$. If the flow is aligned to the x direction, then CFL_x is equal to unity. If the viscous terms are becoming important, the von Neumann number determines the maximum allowable time step

$$\Delta\tau=\Delta y^2/2\nu$$

and CFL_x becomes small.

If the viscous terms are also treated with a line-implicit method in the y direction, then this von Neumann restriction on the time step disappears, and the CFL_x number is again in the order of unity. It is obvious that the acoustic and viscous terms need an implicit treatment in the direction of the smallest grid distances. These parts consist of linear terms. The convective part is nonlinear, and if an explicit treatment is used for this part, no Jacobians have to be recomputed every time step to update the set of equations. An implicit treatment of the convective part on high-aspect-ratio grids is not really necessary because the ratio $(u/\Delta x)/(v/\Delta y)$ can have the same values on an anisotropic grid as on an isotropic grid with more alignment of the flow, where it is known that explicit methods work well, for example, the bump test case. Therefore, our strategy is a combination of an explicit local preconditioning method and an implicit line method for the acoustic and viscous terms in the direction of the smallest grid distances.

This semi-implicit line method for a grid with small cell dimensions in the y direction is given by

$$\Gamma\frac{\partial \boldsymbol{Q}}{\partial \tau}+\frac{\partial F_c^n}{\partial x}+\frac{\partial F_a^n}{\partial x}+\frac{\partial G_c^n}{\partial y}+\frac{\partial G_a^{n+1}}{\partial y}$$
$$-(A_v+A_d)\left(\boldsymbol{Q}_{i-1,j}^n-2\boldsymbol{Q}_{i,j}^{n+1}+\boldsymbol{Q}_{i+1,j}^n\right)$$
$$-(B_v+B_d)\left(\boldsymbol{Q}_{i,j-1}^{n+1}-2\boldsymbol{Q}_{i,j}^{n+1}+\boldsymbol{Q}_{i,j+1}^{n+1}\right)=0 \tag{8}$$

where the matrices A_v, B_v, A_d, and B_d correspond to the viscous and dissipative parts and where

$$\beta=\sqrt{u^2+v^2}+2\nu/\Delta x \tag{9}$$

In Eq. (9) there is no viscous contribution from the y direction, and in Eq. (7) there is no acoustic contribution from the y direction because these terms are treated implicitly in this direction.

Low-Speed Compressible Flow

The described method can easily be extended to viscous low-Mach-number flow. The pseudocompressibility method causes the convective and pseudoacoustic wave speeds to be in the same order of magnitude. Therefore, for compressible flow, any preconditioner can be used that also scales the convective and the acoustic speeds. We choose the preconditioner of Weiss and Smith[1]:

$$\Gamma=\begin{bmatrix}\Theta & 0 & 0 & \rho_T\\ \Theta u & \rho & 0 & \rho_T u\\ \Theta v & 0 & \rho & \rho_T v\\ \Theta H-1 & \rho u & \rho v & \rho_T H+\rho C_p\end{bmatrix} \tag{10}$$

where $\Theta = 1/\beta^2 - \rho_T/\rho C_p$. This preconditioner is used to update the so-called viscous variables: $\boldsymbol{Q}_v = [p \;\; u \;\; v \;\; T]^T$, where T is the temperature and superscript T the transposed vector. Here ρ_T is the derivative of ρ with respect to T.

Again a semi-implicit line method is used in the direction of the smallest grid distances.

Discretization

As for incompressible flows, the convective part of the momentum equation is discretized with velocity upwinding:

$$F_{c_{i+\frac{1}{2}}} = u_{i+\frac{1}{2}}[0 \quad \rho u \quad \rho v \quad 0]^T_{L/R}$$

$$G_{c_{j+\frac{1}{2}}} = v_{j+\frac{1}{2}}[0 \quad \rho u \quad \rho v \quad 0]^T_{L/R}$$

The pressure term in the momentum equations and the velocity terms in the continuity and energy equations are treated in the same way as the pseudoacoustic part for incompressible flow and are discretized centrally.

A stabilization term is added to the mass flux. In the x direction, the mass flux is modified by

$$\tfrac{1}{2}[(p_{i+1} - p_i)/\beta_x + |u|\rho_T(T_{i+1} - T_i)]$$

where β_x is given by Eq. (1). A similar modification is used in the y direction. In the y direction, this term is treated implicitly along a line.

The discretization in pseudotime is done with the preconditioner (10). The acoustic flux is treated implicitly in the direction of the shortest grid distances. Because this flux is nonlinear in the compressible case, a linearization is needed. The acoustic flux on time level $n+1$ is written as

$$G^{n+1}_{a_{j+\frac{1}{2}}} = \begin{bmatrix} \rho^n v^{n+1} \\ 0 \\ p^{n+1} \\ \rho^n H^n v^{n+1} \end{bmatrix}_{j+\frac{1}{2}}$$

Finally, the normal viscous fluxes are treated implicitly. The tangential viscous fluxes are treated explicitly.

Viscous Low-Speed Flow

Backward-Facing Step Flow

The method is tested on a backward-facing step problem. The height of the step is chosen as one-third of the channel height. We consider two grids. The first grid has 81×49 nodes, and the second grid has 81×193 nodes. Both grids have the same distribution of points in the x direction. In the y direction, the second grid has four times more cells than the first one. The highest aspect ratio on the first grid is about 35 and on the second grid 140. The CFL number is set to 1.8.

Figure 1 shows the streamline pattern obtained on the first grid for a Reynolds number $Re_h = (U_{\max} h)/\nu = 150$, where h is the height of the step and $U_{\max}$ is the maximum value of the velocity at the inlet section. Figure 2 shows the convergence history for the multigrid (MG) line method on the two grids with different grid aspect ratios and for different inflow Mach numbers. It is clear that neither the grid aspect ratio nor the Mach number has any influence on the performance of the method.

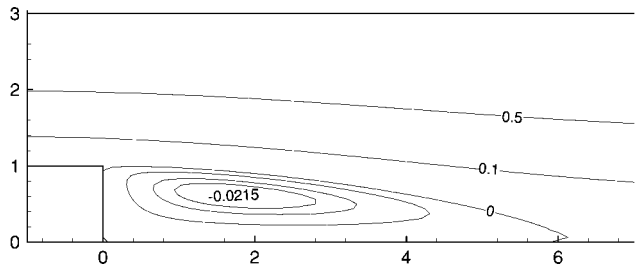

Fig. 1 Streamline pattern for the backward-facing step problem, obtained at the finest grid.

Table 1 Nusselt numbers on the hot and cold wall and their mean value compared and extrapolated with Richardson's method (h = 1/1024) for $Ra = 10^6$ for different grid sizes

N	$\overline{Nu_h}$	$\overline{Nu_c}$	$\overline{Nu}_{\text{mean}}$	%error
256	8.686670690	8.685418776	8.686044733	0.00623
512	8.686602534	8.686279239	8.686440887	0.00167
512 ($AR = 1000$)	8.687212911	8.687192546	8.686202729	0.00710
1024	8.686588147	8.686505978	8.686547062	0.00045
Richardson extrapolation	8.686584298	8.686587101	8.686585939	——
α	−2.244094219	−1.924085864	−1.899606003	——
C	6.76085E−13	−1.30940E−10	−7.43535E−11	——

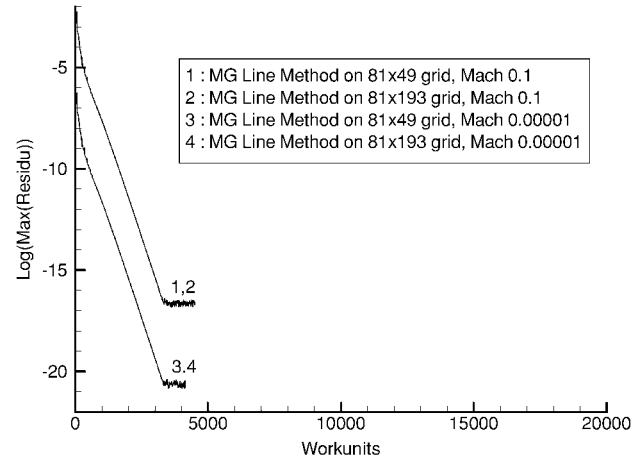

Fig. 2 Convergence results for the compressible backward-facing step problem, comparison of the MG line method on two different grids for different Mach numbers.

Flow in Thermally Driven Cavity

This test problem considers a buoyancy-driven flow in a square cavity.[4,9] The configuration consists of two vertical walls at temperature T_h and T_c and two adiabatic horizontal walls. It is known that this problem exhibits complex flow features depending on the Rayleigh number $[Ra = \rho^2 g\beta(T_h - T_c)L^3 C_p/\mu k]$, the aspect ratio of the cavity, and a temperature difference parameter $[\varepsilon = (T_h - T_c)/(T_h + T_c)]$. Here β is the thermal expansion coefficient, g is the magnitude of the gravitational field, L is the length of the cavity walls, and μ and k are the dynamic viscosity and thermal conductivity, respectively.

For the present study, three Rayleigh numbers, $Ra = 10^3$, 10^5, and 10^6, are considered with a temperature difference parameter $\varepsilon = 0.6$. In the corners the grid aspect ratio is one. From there the grid is stretched toward the center. Grid sizes of 256×256, 512×512 and 1024×1024 are used. The maximum aspect ratio is 80 in both directions for all grids. For the 256×256 grid, the stretching factor is adapted so that also a grid is obtained with maximum aspect ratio of 1000 in both directions. The transport properties (μ and k) are evaluated by using Sutherland's law (see Ref. 9). The Prandtl number based on reference transport properties is 0.71. A local reference velocity w_r for the pressure dissipation term is used for all cases. Figure 3 shows temperature isolines and streamlines for $Ra = 10^3$, 10^5, and 10^6.

For the $Ra = 10^6$ case, a grid refinement study is performed. The results are summarized in Table 1. The extrapolated values are computed with Richardson's extrapolation method:

$$f_{\text{extrapol}} = f_h - Ch^\alpha$$

where

$$\alpha = \frac{\ln[(f_h - f_{h/2})/(f_{h/2} - f_{h/4})]}{\ln(2)}$$

$$C = \frac{f_h - f_{h/2}}{h^\alpha(1 - 2^{-\alpha})}$$

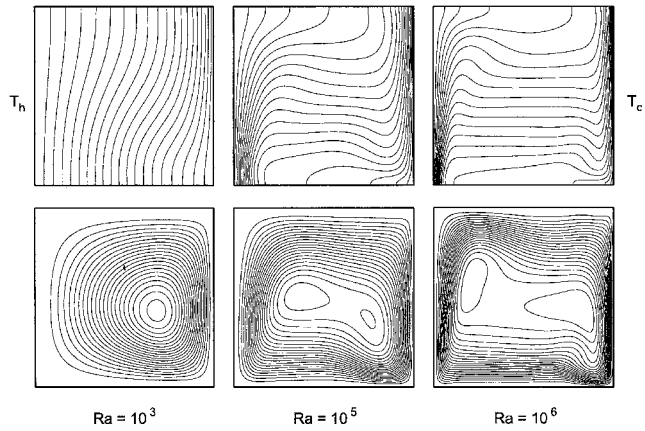

Fig. 3 Temperature isolines and streamlines for a viscous flow in a thermally driven cavity for $Ra = 10^3$, 10^5, and 10^6.

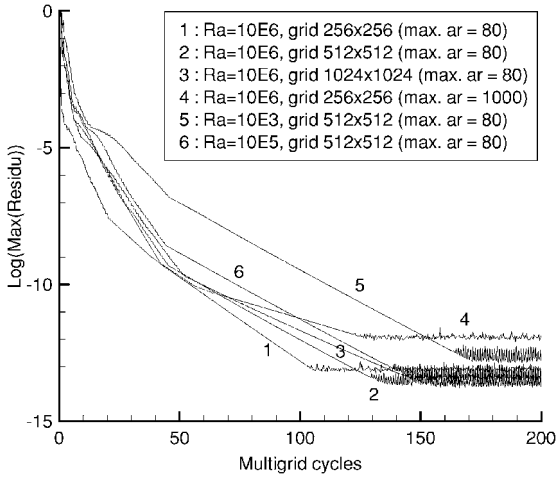

Fig. 4 Convergence results for the thermally driven cavity flow problem with $Ra = 10^3$, 10^5, and 10^6 for different grid sizes with different grid aspect ratios.

where h is given by $1/N$, where N is the number of grid cells in one direction. We used the method with $h = 1/1024$. The computed α values show that quadratic grid convergence is obtained. The Nusselt values are in agreement with values given by Chenoweth and Paolucci.[9] The calculation on the grid with maximum aspect ratio of 1000 gives a less accurate result because the grid is too coarse in the center of the cavity.

The convergence behavior is shown in Fig. 4, showing that the convergence rate does not depend on the Rayleigh number or on the grid aspect ratio.

Blending to the AUSM+ Scheme

The AUSM+ scheme[6] has been used as discretization scheme for high-speed flows. In this method the inviscid interface flux $F_{i+1/2}$ in the x direction is split into a convective contribution $F_{c_{i+1/2}}$ and a pressure contribution $F_{p_{i+1/2}}$:

$$F_c = (\rho u)_{i+\frac{1}{2}} \begin{bmatrix} 1 \\ u \\ v \\ H \end{bmatrix}_{L/R}, \qquad F_p = \begin{bmatrix} 0 \\ p_{i+\frac{1}{2}} \\ 0 \\ 0 \end{bmatrix} \tag{11}$$

where state L is chosen if $(\rho u)_{i+1/2}$ is nonnegative and state R is chosen if $(\rho u)_{i+1/2}$ is negative.

To operate the scheme at all Mach numbers, a blending of the low-speed flux F^{LS} and high-speed flux $F^{\mathrm{AUSM+}}$ definitions is needed:

$$F = (1-\alpha)F^{\mathrm{AUSM+}} + \alpha F^{\mathrm{LS}}$$

with

$$\alpha = \begin{cases} 0, & \left|M_{i+\frac{1}{2}}\right| > M_{\mathrm{bl}} \\ 1 - \left|M_{i+\frac{1}{2}}\right| / M_{\mathrm{bl}} & \\ \quad + (1/2\pi)\sin\left(2\pi \left|M_{i+\frac{1}{2}}\right| / M_{\mathrm{bl}}\right), & \text{otherwise} \end{cases}$$

M_{bl} is chosen as 0.5. With this blending function, the first and second derivatives of F are continuous in the whole Mach number range. We remark that the low Mach number limit of the convective part of the AUSM+ scheme is given by

$$F_{c_{i+\frac{1}{2}}} = u_{i+\frac{1}{2}}[\rho \quad \rho u \quad \rho v \quad \rho H]^T_{L/R}$$

$$G_{c_{j+\frac{1}{2}}} = v_{j+\frac{1}{2}}[\rho \quad \rho u \quad \rho v \quad \rho H]^T_{L/R}$$

This is almost the same discretization as we used for the low-Mach-number scheme. Therefore, to avoid too much computational effort, we changed the low-Mach-number discretization for the convective part and the velocity terms in the acoustic part so that it corresponds with the AUSM+ convective part. Because of the upwinding of the enthalpy, only a pressure stabilization is necessary now in the mass flux, so that the temperature part could be left out. A similar pressure–velocity coupling is also introduced in Ref. 6.

The resulting flux is given by Eq. (11) with

$$(\rho u)_{i+\frac{1}{2}} = (\rho u)^{\mathrm{AUSM+}}_{i+\frac{1}{2}} - (\alpha/2\beta_x)(p_R - p_L)$$

$$p_{i+\frac{1}{2}} = (1-\alpha)p^{\mathrm{AUSM+}}_{i+\frac{1}{2}} + \alpha[(p_i + p_{i+1})/2]$$

The preconditioner is only affected by a change of β:

$$\beta = (1-\alpha)c + \alpha\beta^{\mathrm{LS}} \tag{12}$$

where c is the speed of sound. For $\alpha = 0$, β becomes equal to c, which corresponds with no preconditioning. The time step is computed according to Eq. (5) with

$$c_y = (1-\alpha)c'_y + \alpha|v| \tag{13}$$

where c'_y is given by Eq. (6). Only the part of the low-speed flux is treated implicitly along lines in the direction of the shortest grid distance in the same way as it is done for low-speed compressible flow.

Inviscid Flow Past a Bump

Calculations are done for flow in a channel with a bump perturbation in the bottom wall and for inlet Mach numbers 0.001, 0.1, 0.85, and 2. This means for flows ranging from low-Mach-number subsonic to transonic and supersonic flows. Because for the transonic and the supersonic flows shocks occur, the second-order formulation for the convective terms has to be changed to a total variation diminishing formulation. The minmod limiter is used. For such a nonlinear scheme, the multistage stepping has to be adjusted. A five-step multistage stepping algorithm is used with coefficients 1, 0.576, 0.307, 0.16, 0.066, and CFL equal to 1.55 (Ref. 10). In the MG formulation, implicit residual weighting of the residuals is done before restriction from a finer to a coarser grid, and on coarse grids, first-order discretization is used for the convective terms.[10] The fine grid has in all cases 48×16 cells. Three levels of grids are used with one presmoothing and one postsmoothing. Figure 5 shows the obtained Mach number contours. For the two low-Mach-number flows, flow patterns are identical.

Convergence histories are shown in Fig. 6. The low subsonic flow regimes show a flow-independent convergence rate. The $M_\infty = 0.001$ calculation levels out due to roundoff errors after a residual reduction of seven orders of magnitude. The transonic flow calculation has the slowest convergence. The supersonic cases shows fast convergence behavior as expected. As is well known, the lower convergence rate for the transonic flow case is due to the

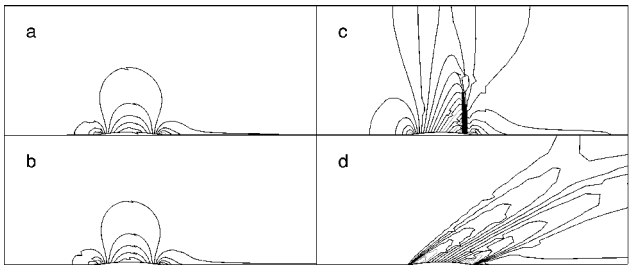

Fig. 5 Mach number contours for the second-order scheme: a) $M_\infty = 0.001$, b) $M_\infty = 0.1$, c) $M_\infty = 0.85$, and d) $M_\infty = 2$.

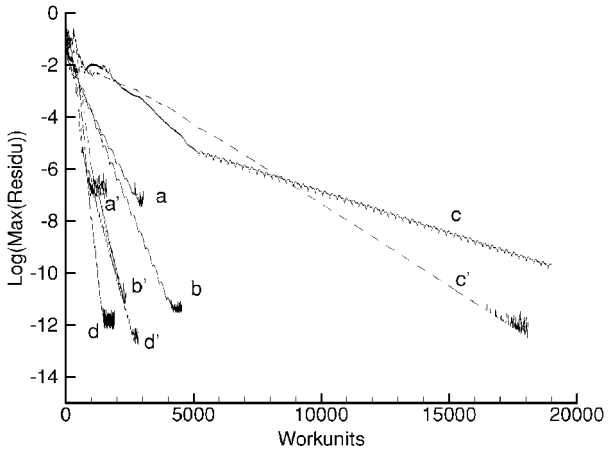

Fig. 6 Convergence histories for the second-order scheme, where a is $M_\infty = 0.001$, b is $M_\infty = 0.1$, c is $M_\infty = 0.85$, and d is $M_\infty = 2$; prime denotes computations on a grid with four time more cells in the direction normal to the bump.

stiffness of the combined convective-acoustic terms in the longitudinal direction, because the flow velocity becomes equal to sound velocity on the sonic line. To improve the convergence speed, an implicit time stepping has to be used. We did not implement an implicit time stepping here. The test cases shown in Fig. 5 are meant to demonstrate that the blending with the AUSM+ scheme works well and that the convergence speed for the low-Mach-number flows remains independent of Mach number after the adjustment necessary for blending. Furthermore, we want to demonstrate that the convergence speed is not dependent on grid aspect ratio. With respect to this feature, note that, for all flows shown in Fig. 5, in the transversal direction the low-speed fluxes are used and that the time stepping is implicit on vertical lines for the acoustic terms and for the dissipation terms.

The influence of a change in grid aspect ratio (four times) is shown in Fig. 6. The convergence histories denoted with the prime have almost the same behavior as those for the grid with smaller grid aspect ratio. We think that the small differences in convergence behavior are due to the change of angle between velocity and grid lines in the computational space. For the low-Mach-number flows, there is better convergence for the grid with the higher aspect ratio. This would not have been the case without the use of a line smoother.

Conclusions

A method of discretization of the incompressible and low-Mach-number compressible Navier–Stokes equations is presented. The local preconditioning method is combined with a line solver to remove the stiffness coming from high grid aspect ratios. This line solver is used in a multistage stepping scheme and accelerated with the MG method. Different test cases show that the accuracy of the discretization method is very good. The convergence of the solution method is very fast for both incompressible and low-Mach-number compressible flows, independent of the grid aspect ratio.

The method is extended toward high-Mach-number flows with a blending to the AUSM+ scheme. The solution and the convergence behavior are now dependent on the Mach number. The transonic case showed the slowest convergence rate. No negative influence of grid aspect ratio could be observed thanks to the use of the line method.

References

[1]Weiss, J., and Smith, W., "Preconditioning Applied to Variable and Constant Density Flows," *AIAA Journal*, Vol. 33, No. 11, 1995, pp. 2050–2057.

[2]Turkel, E., "Preconditioning Techniques in Computational Fluid Dynamics," *Annual Review of Fluid Mechanics*, Vol. 31, 1999, pp. 385–416.

[3]Lee, D., van Leer, B., and Lynn, J., "A Local Navier–Stokes Preconditioner for All Mach and Cell Reynolds Numbers," *Proceedings of the 13th AIAA Computational Fluid Dynamics Conference*, AIAA, Reston, VA, 1997, pp. 842–855.

[4]Choi, Y., and Merkle, C., "The Application of Preconditioning in Viscous Flows," *Journal of Computational Physics*, Vol. 105, 1993, pp. 207–223.

[5]Liou, M.-S., and Steffen, C. J., Jr., "A New Flux Splitting Scheme," *Journal of Computational Physics*, Vol. 107, 1993, pp. 23–39.

[6]Edwards, J., and Liou, M.-S., "Low-Diffusion Flux Splitting Methods for Flows at All Speeds," *AIAA Journal*, Vol. 36, No. 9, 1998, pp. 1610–1617.

[7]van Leer, B., "Toward the Ultimate Conservative Difference Scheme. III. Upstream-Centered Finite-Difference Schemes for Ideal Compressible Flow," *Journal of Computational Physics*, Vol. 23, 1997, pp. 263–275.

[8]Vierendeels, J., Riemslagh, K., and Dick, E., "A Multigrid Semi-Implicit Line-Method for Viscous Incompressible and Low-Mach-Number Flows on High Aspect Ratio Grids," *Journal of Computational Physics*, Vol. 154, 1999, pp. 310–341.

[9]Chenoweth, D. R., and Paolucci, S., "Natural Convection in an Enclosed Vertical Air Layer with Large Horizontal Temperature Differences," *Journal of Fluid Mechanics*, Vol. 169, 1986, pp. 173–210.

[10]Dick, E., and Riemslagh, K., "Multi-Staging of Jacobi Relaxation in Multigrid Methods for Steady Euler Equations, II," *Journal of Computational and Applied Mathematics*, Vol. 59, 1995, pp. 339–348.

J. Kallinderis
Associate Editor